One-Shot Learning of Human Activity With an MAP Adapted GMM and Simplex-HMM

Mario Rodriguez, Carlos Orrite, *Member, IEEE*, Carlos Medrano, *Senior Member, IEEE*, and Dimitrios Makris, *Member, IEEE*

***Abstract*—This paper presents a novel activity class representation using a single sequence for training. The contribution of this representation lays on the ability to train an one-shot learning recognition system, useful in new scenarios where capturing and labeling sequences is expensive or impractical. The method uses a universal background model of local descriptors obtained from source databases available on-line and adapts it to a new sequence in the target scenario through a maximum *a posteriori* adaptation. Each activity sample is encoded in a sequence of normalized bag of features and modeled by a new hidden Markov model formulation, where the expectation-maximization algorithm for training is modified to deal with observations consisting in vectors in a unit simplex. Extensive experiments in recognition have been performed using one-shot learning over the public datasets Weizmann, KTH, and IXMAS. These experiments demonstrate the discriminative properties of the representation and the validity of application in recognition systems, achieving state-of-the-art results.**

***Index Terms*—Activity recognition, hidden Markov model (HMM), maximum *a posteriori* (MAP) adaptation, soft-assignment, transfer learning.**

I. Introduction

MACHINE learning advances in video-based human activity recognition and the ubiquity presence of video cameras in our daily life have inspired multiple application areas such as search engines, indexing, surveillance, entertainment, and home automation. However, further research in action recognition is required to achieve commercially acceptable reliability.

Most of the proposed recognition approaches are trained with large amount of labeled examples using large databases and usually validating the method with leave-one-out or train-test split strategies. In practice, this is reasonable for applications with unconstrained scenarios such as searching specific activities in movies, or indexing Internet videos, where the training examples can be obtained relatively easy from online videos. Results in large and unconstrained datasets such as HMDB51 [1] or OlympicSports [2] are useful for general evaluation, because their examples have been collected from diverse sources, for instance YouTube or extracted from movies, but accuracy of algorithms is not yet at the level required in many commercial applications.

Higher accuracy can be achieved in constrained scenarios and with fixed cameras, such as the ones represented by the Weizmann [3], KTH [4], or IXMAS [5] datasets, assuming the availability of several labeled examples for training.

Recognizing in a fixed scenario has the advantage of suppressing in some degree the clutter introduced by the change of background and viewpoint and therefore higher reliability may be achieved. Many applications, such as visual monitoring of elderly or disabled people at home, video surveillance or gaming, can be considered that are similarly constrained, assuming that they were installed in a specific environment. However, after the installation, the system should be retrained again as any previously collected sequences may not be representative of the new environment. Although the performance is constrained by the number of labeled sequences used for training, collecting, and labeling large amount of data for the particular scenario is infeasible, as it is laborious and may require the involvement of the user. Little research has been done in training an activity recognition system with limited number of labeled examples although being an essential feature in many practical situations [6]–[9].

In the ideal case, only one sequence per class should be enough for activity representation as shown in some previous work [6]. However, it is important to mention that the description of an one-shot learning approach differs among papers in the literature. In order to have a better understanding of the meaning we classify the different approaches into two groups. First, the strict one-shot learning assumes only one training example available which is used to model a single class. After training several models (one per available example) of different classes separately, it is possible to combine these models in order to train a recognition systems. Seo and Milanfar [6] proposed a nearest-neighbor classification using a strict one-shot learning approach. Second, the relaxed one-shot learning process uses simultaneously multiple training examples available, assuming one per class. This relaxation allows sharing some information among the examples in order to model the

Manuscript received January 8, 2016; revised April 11, 2016; accepted April 12, 2016. Date of publication May 10, 2016; date of current version June 14, 2017. This work was supported in part by the Spanish Grant TIN2013-45312-R (MINECO), Gobierno de Aragon, and in part by the European Social Fund. The work of M. Rodriguez was supported by the Spanish FPI under Grant BES-2011-043752 and Grant EEBB-I-14-08410. This paper was recommended by Associate Editor J. Su.

M. Rodriguez and C. Orrite are with the CV Laboratory, Aragon Institute for Engineering Research, Zaragoza University, Zaragoza 50018, Spain (e-mail: mrodrigo@unizar.es).

C. Medrano is with the EduQTech, E.U. Politecnica, Zaragoza University, Teruel 44003, Spain.

D. Makris is with the Digital Imaging Research Centre, Kingston University, Kingston upon Thames KT1 2EE, U.K.

Color versions of one or more of the figures in this paper are available online at http://ieeexplore.ieee.org.

Digital Object Identifier 10.1109/TCYB.2016.2558447

2168-2267 © 2016 IEEE. Personal use is permitted, but republication/redistribution requires IEEE permission.
See http://www.ieee.org/publications_standards/publications/rights/index.html for more information.

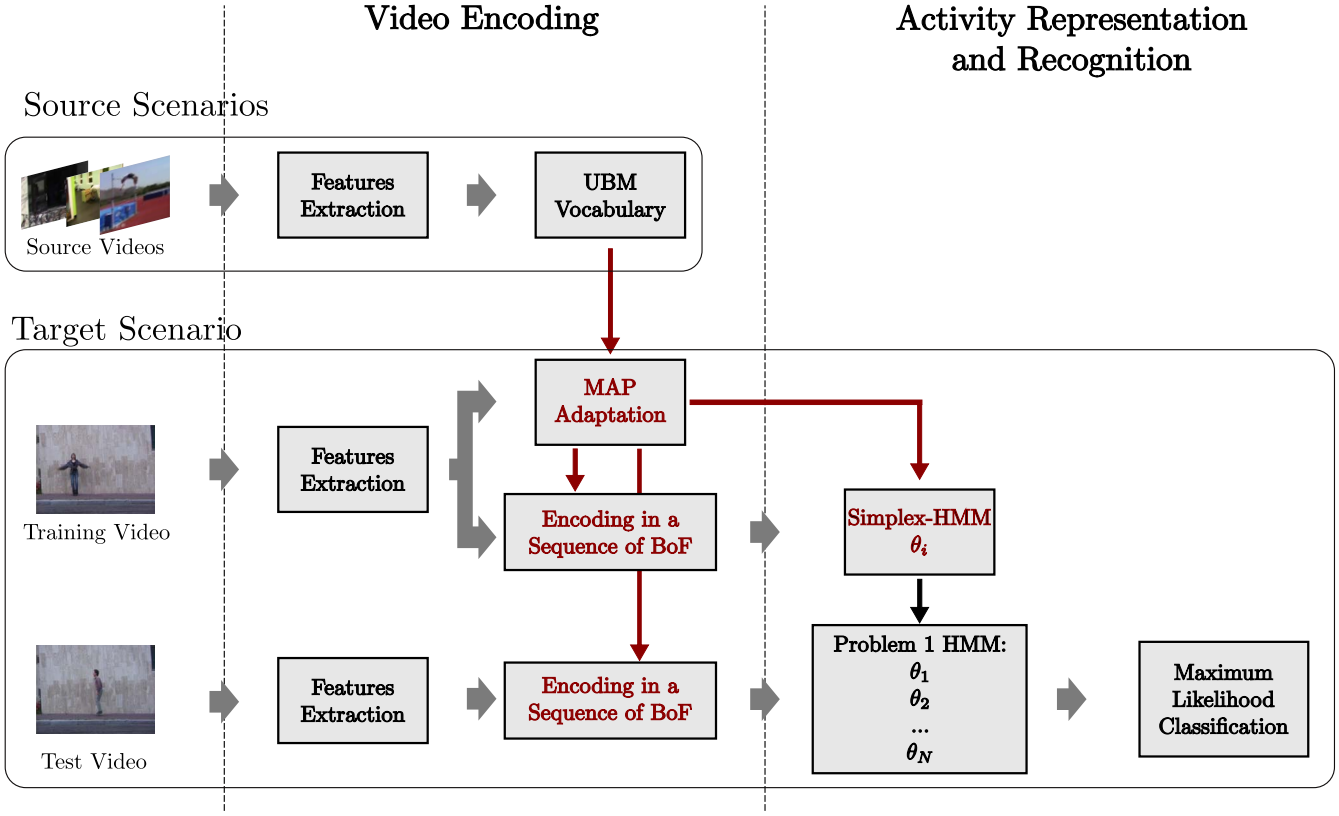

Fig. 1. Flow diagram of the proposed approach, highlighting in red the stages where the main novelties are introduced. Video encoding is explained in Section III and activity representation and recognition are explained in Section IV.

classes or directly training a recognition system. Methods by Yang *et al.* [7] and Orrite *et al.* [8] follow this description as they create a vocabulary of features using sequences of the different classes. The relaxed approach usually gives better results but at the expense of retraining the system with each new inclusion and with the inconvenience of requiring several examples from the beginning. In [9], although Rodríguez *et al.* initially created a vocabulary with sequences of five classes, implying a relaxed model, they used a transfer learning stage to allow the inclusion of new classes without a retraining of the system in a hybrid approach.

In the most restricted scenario just one labeled sequence is available and its activity class should be trained from one example. To carry out with this restriction we propose in this paper the transfer learning of a universal background model (UBM) [10] trained with extensive datasets available on-line, representing the vocabulary of a bag of feature (BoF) model, to the target scenario where only a few labeled sequences are available, and training a specially designed case of a hidden Markov model (HMM).

A flow diagram of the proposed approach is depicted in Fig. 1. From the wide range of features extractors available in the literature, improved dense trajectories (IDTs) [11] have shown state-of-the-art performance in several challenging datasets and so we use them in the features extraction stage. The IDTs are represented by the trajectory of spatio-temporal interest points during a window of time, the histogram of oriented gradients and histogram of optical flow [12] and the motion boundary histograms [13] features in the surrounding spatio-temporal cuboid of the trajectory. The proposed method extracts the IDTs from videos in public datasets of human activities, considered the source domain, and creates a UBM vocabulary modeled with a Gaussian mixture model (GMM) as done in [10], representing general, person and scenario independent features. Unlike [10], the trained UBM represents a universe of features, and not a universe of activities (or speakers in their case). Once selected the target scenario, an initial labeled training video is recorded. The corresponding IDTs are extracted from this video and used in a twofold task. First, with the unordered IDTs, the UBM vocabulary is transferred to the target scenario using a maximum *a posteriori* (MAP) adaptation, and obtaining a sequence specific vocabulary. Second, the IDTs are grouped into temporal windows where they are soft-assigned to the adapted vocabulary, obtaining a BoFs per window. The BoF histogram is normalized so that it sums one, equivalent to say it belongs to a unit simplex. This way, the video is encoded as a sequence of BoF, and the activity is then modeled with an HMM which is a well known generative approach applied on time series.

The expectation-maximization (EM) algorithm is used to solve the difficult task of estimating an HMM. A complication with the EM algorithm is that there is in general no guarantee of reaching a global optimum, and local optima can at times be problematic, particularly with small training sets. Moreover, small training sets produce overfitting as we increase the number of parameters to train and the usual continuous HMM approach that incorporates GMM distributions may lead to an unstable EM algorithm [14]. In order to obtain a reliable

system, the proposed simplex-HMM (SHMM) is numerically stable, even with a single training sequence. Besides, the soft assignment that leads to BoF seems more suitable than a hard assignment for the case of scarce training data.

Testing follows a process flow similar to training. First the IDTs are extracted and a sequence of BoFs is obtained using a temporal sliding window. The encoded video is then evaluated, given the HMM, as described in [15]. Maximum likelihood classification is used to identify the model that fits better the observation and therefore assign an action label. Using the defined one-shot learning system we have obtained state-of-the-art results in the public datasets Weizmann, KTH, and IXMAS.

The two main contributions of this paper are summarized as follows.

1) We propose a new approach for video encoding based on transfer learning where a UBM vocabulary is obtained training a GMM with features from every sequence in the source domain, and adapted to the feature space extracted from the target scenario by an MAP adaptation of the GMM conforming a target domain vocabulary.
2) We define an HMM constrained to a sequence of vectors in a simplex (SHMM), avoiding the numerical problems produced in the HMM training with scarce data.

The rest of this paper is divided in the following sections. In Section II, a brief review of related research is given. In Section III, the video encoding is explained, using the UBM adapted to the target domain. Section IV describes the SHMM. The experimental results are shown in Section V. Finally, a discussion of this paper is done in Section VI.

II. Related Work

A large volume of human activity recognition research has been performed in the last decades, mainly attempting to address two important questions: 1) feature extraction and 2) activity classification [16]–[18].

Many methods have been proposed for feature extraction, ranging from global to local descriptors. Global descriptors provide an holistic representation, while local descriptors usually use some encoding to reach that holistic representation. A single global descriptor encodes the activity by detecting a region of interest through a bounding box or a contour where the person performs the activity. Examples of these approaches use human silhouettes to create motion history images (MHIs) and motion energy images [19], [20], track the body contours creating spatio-temporal shapes [21] or obtain spatio-temporal volumes spanned by silhouette images [3]. Although they encode powerfully the activity information, they rely on accurate localization, background subtraction or tracking, being more sensitive to viewpoint, illumination changes, noise, and occlusions. On the other side of the spectrum, the local descriptors are computed in small spatio-temporal volumes around interest points. Some descriptors only encode the image appearance [22], but usually spatio-temporal descriptors show better performance [12], [23]–[25]. The most common encoding of the extracted descriptors in a video activity is BoF representation, although recent state-of-the-art works have improved the results using Fisher vectors (FVs) [26]. Methods based on local descriptors are robust to occlusion and are less dependent on viewpoint and illumination changes. However, they are too local and the encodings overlook important spatial and long-term temporal information. Recent approaches have obtain state-of-the-art results by expanding the local features to hybrid models where the spatio-temporal interest points are tracked during some frames obtaining a trajectory around which the descriptor is computed [11], [27].

Once the feature vectors are extracted, the recognition process becomes a classification problem. Several methodologies have been employed being discriminative or generative, considering or overlooking the temporal domain. A direct classification is performed selecting the class of the nearest neighbor (NN), the class of the closest training sequence. In order to avoid noise the k-NN methodology selects the most common label of the k closest sequences [20], [28]. Some methods consider the temporal domain to compute the distance, as dynamic time warping do [29], [30]. A widely used discriminative model is the support vector machine (SVM) that learns an hyperplane in feature space that discriminates between two classes [4], [11]. SVM can be combined with BoF or FV losing the long-term temporal information in the encoding. On the other hand, some discriminative methods take into account this information as conditional random fields (CRFs) [31], [32] and its evolution hidden CRF [33] do. The use of discriminative methods is not suitable for a strict one-shot learning approach as the method should be able to perform the training from a single example, so a generative method is needed. HMM is a generative method widely used in classification on time series [15], [34], [35].

The usual EM training process of HMM fails when training with a short number of examples and different strategies can be adopted in order to minimize the problem. Previous work has shown how an HMM modification called fuzzy discrete HMM (FDHMM) exploits a soft-assignment in a discrete HMM [36], obtaining a stable training with scarce data. Its application in activity recognition improves the performance [8] in a relaxed one-shot learning scenario, and the method can benefit from a transfer learning process [9]. In the last few years, transfer learning applied in human activity recognition has attracted the interest of researchers, as reflected in recent surveys [37], [38]. It is based on the use of external information from a source domain that complements the limited data available in a target domain where the recognition task is implemented. Liu *et al.* [39] used an interlingua in order to merge data from source domains and target domain, considering labeled data available only in the source domain, which classifies their method as uninformed supervised (U.S.). In [40], a similar approach is implemented by creating a cross-domain codebook where labeled actions from both domains are modeled with BoF, being an informed supervised transfer learning method. Zhu *et al.* [41] created a codebook with unlabeled data from the source domain and train the recognition with labeled data from the target domain, being an informed unsupervised transfer learning method. The literature is really extensive, but most of the methods use similar approaches [42], [43]. The UBM vocabulary adaptation

proposed in this paper lays in the U.S. transfer learning as the source domain descriptors are labeled in a GMM training process and this GMM is later adapted to unlabeled target domain descriptors. A novelty introduced by this paper is the transfer learning per sequence, and specifically the adaptation of the UBM to as many vocabularies as labeled sequences in the target domain.

III. Video Encoding

Following the diagram depicted in the video encoding section of Fig. 1, video encoding comprises two different tasks. First, a UBM is modeled by a GMM using source videos, widely available, and afterwards, the adaptation of this UBM–GMM takes place on the target scenario. Second, as the video is encoded in a BoF taken into account a codebook, where the temporal information of the activity is lost, a temporal sliding window is used to recover this kind of information.

Next, we describe the temporal activity model by a GMM following a soft-assignment to a BoF approach. Later, we introduce the modification of the UBM vocabulary based on U.S. transfer learning. Finally, we explain the motivation for using a sliding window to code temporal information given as a result a sequence of observations that will be used for training an HMM.

A. Soft-Assignment-BoF

Over the past several years, many methods have modeled activities by encoding the extracted features in a single BoF, obtaining the codebook bins through a clustering algorithm of the training samples. Two of the most common clustering algorithms are *k*-means, which creates a Voronoi tessellation, and GMM, optimized with an EM process. The former is defined only by the mean while the latter encodes second-order information as includes both, the mean and the covariance and even a weight of the cluster. The proposed encoding uses the IDT features extracted from the activity videos and models the features space through a GMM. The number of clusters K can vary a lot in different approaches and empirically has been proven that a large number, in the order of thousands, is appropriate for BoF encoding [27], while FV allows a smaller number of Gaussians, in the order of hundreds [11].

From each video activity, a set of IDT feature vectors $\mathbf{Q} = \{\mathbf{q}_j\}$, $\mathbf{q}_j \in \mathbb{R}^D$ is extracted. Using the feature vectors of the training examples a GMM, $\lambda = \{\omega_i, \mu_i, \Sigma_i\}$, is calculated through an EM process. The general model of GMM supports full covariance matrices, but diagonal covariance matrices can satisfactorily approximate the original density modeling with a higher order GMM and they are computationally more efficient. Therefore, the framework uses diagonal covariance matrices and in addition it disregards GMM weights obtaining a simplified model $\lambda = \{\mu_i, \Sigma_i\}$.

Fig. 2 shows a sample evaluated in every Gaussian of the GMM used to encode the data in a soft-assignment-BoF. Using the simplified GMM, $\lambda = \{\mu_i, \Sigma_i\}$, the activity in a video is encoded with a BoF where each bin value v_{λ_i} is calculated by proportionally adding the contributions of every extracted feature $\mathbf{q}_j$ to the specific Gaussian λ_i, as expressed in (1),

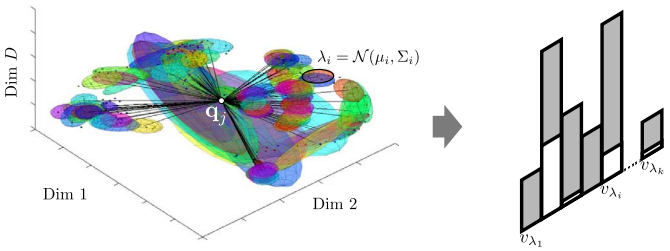

Fig. 2. GMM representation and soft-assignment-BoF. Gray bars represents the BoF while white highlighted bars represents the $\mathbf{q}_j$ sample contribution.

where M is the number of features extracted, and K is the number of Gaussians in the GMM

$$v_{\lambda_i} = \frac{1}{M}\sum_{j=1}^{M} p(\lambda_i|\mathbf{q}_j) = \frac{1}{M}\sum_{j=1}^{M} \frac{\mathcal{N}(\mathbf{q}_j; \mu_i, \Sigma_i)}{\sum_{k=1}^{K}\mathcal{N}(\mathbf{q}_j; \mu_k, \Sigma_k)}. \quad (1)$$

Thanks to the applied normalizations $\sum_{k=1}^{K} p(\lambda_k|\mathbf{q}_j) = 1$ every BoF vector belongs to the unit simplex $\Delta = \{\mathbf{v}_\lambda \in \mathbb{R}^K : v_{\lambda_i} \geq 0 : \sum_{k=1}^{K} v_{\lambda_k} = 1\}$.

With many feature samples, the proposed soft-assignment is unnecessary and the winner-takes-all rule usually applied in BoF approaches is sufficient. However, the one-shot learning objective is to obtain a representative model with only one activity example which contains few feature samples, therefore keeping as much information as possible, as a proper soft-assignment does, is essential.

B. Transfer Learning With MAP Adaptation

In addition to the soft-assignment-BoF designed to deal with scarce data, another problem arises from the need of a codebook trained with the same scarce data, clearly insufficient using only one video activity example.

As mentioned before, although few samples are available in the target domain, plenty of videos can be obtained on-line as source domain from where the learning is transferred to the target domain. Several machine learning methods have used the approach of transfer learning from a source domain to a target domain. Especially, successful have been the speaker verification systems based on UBM–GMM [10], although they transferred the class model and not a vocabulary. As previous research has proven, target domain information improves recognition system performance [9], [44].

Fig. 3 represents the proposed transfer learning process showing a simplified 2-D GMM trained in the source domain and adapted to the target domain. From the source domain a large number of IDTs is randomly extracted $\mathbf{S} = \{\mathbf{s}_j\}$, $\mathbf{s}_i \in \mathbb{R}^D$, being unlabeled data, and then used in an EM process to train the GMM which represents the UBM, $\lambda = \{\mu_i, \Sigma_i\}$. This UBM is later MAP adapted [10] to the target domain using only the available samples in this domain, they can be as few as the extracted from a single sequence, $\mathbf{Q} = \{\mathbf{q}_j\}$, $\mathbf{q}_j \in \mathbb{R}^D$. For Gaussian λ_i in the UBM, the probabilistic alignment of the feature vectors is computed with

$$p(\lambda_i|\mathbf{q}_j) = \frac{\mathcal{N}(\mathbf{q}_j; \mu_i, \Sigma_i)}{\sum_{k=1}^{K}\mathcal{N}(\mathbf{q}_j; \mu_k, \Sigma_k)}. \quad (2)$$

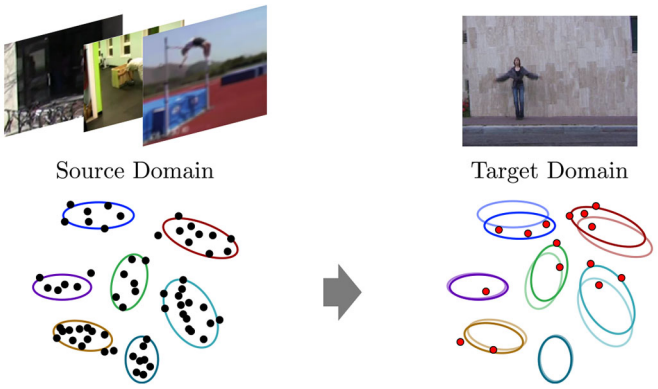

Fig. 3. Source GMM and MAP adapted GMM.

These probabilistic alignments and the features vectors are used to compute the sufficient statistics of the mean with (3) and (4). Weights have been disregarded so every Gaussian has the same weight, and covariance adaptation has been proven to be dispensable in most of the systems, so the system keeps the original covariance matrices in every new adapted GMM

$$n_i = \sum_{j=1}^{M} p(\lambda_i|\mathbf{q}_j) \tag{3}$$

$$E_i(\mathbf{Q}) = \frac{1}{n_i}\sum_{j=1}^{M} p(\lambda_i|\mathbf{q}_j)\mathbf{q}_j. \tag{4}$$

The sufficient statistics, computed with the target domain training data, are used to update the UBM, estimating the new means with

$$\widehat{\mu}_i = \alpha_i E_i(\mathbf{Q}) + (1-\alpha_i)\mu_i. \tag{5}$$

The parameter α_i $(0 \leq \alpha_i \leq 1)$ is an adaptation coefficient controlling the balance between old and new estimates that can also be estimated through

$$\alpha_i = \frac{n_i}{n_i + rM} \tag{6}$$

where r is the controlling variable for adaptation and the rM term assures an equal adaptation independent on the number of IDT samples per example. After the MAP adaptation, a new GMM is obtained per video activity, $\widehat{\lambda} = \{\widehat{\mu}_i, \Sigma_i\}$, representing the new codebook used in the encoding.

C. Temporal Sliding Window

The former BoF video encoding loses the long-term temporal information of the activity, disregarding representative data. Therefore, a temporally windowed soft-assignment-BoF encoding is proposed, shown in Fig. 4. The MAP adaptation of the UBM vocabulary to the target scenario is performed with the features extracted from the whole video, as done before. On the other hand, every N_w frames a new BoF is obtained, keeping the long-term temporal information in a sequence of BoF, $\mathcal{O} = \{O_1, \ldots, O_T\}$. The encoding uses IDT as descriptors which are computed through a temporal window of length N_l, generally different to N_w. Each IDT, $\mathbf{q}_j$, has

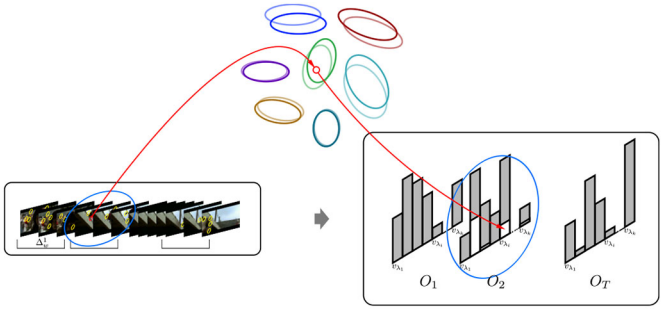

Fig. 4. BoF sequence of windowed video.

associated a temporal window Δ_l^j and influences proportionally to each Δ_w^t window

$$\rho_{jt} = \frac{\left|\Delta_w^t \cap \Delta_l^j\right|}{N_w}. \tag{7}$$

Each bin value, $v_{\lambda_i}^t$, associates to a specific BoF, O_t, is then calculated using

$$v_{\lambda_i}^t = \frac{1}{\sum_{j=1}^{M}\rho_{jt}}\sum_{j=1}^{M}\frac{\rho_{jt}\mathcal{N}(\mathbf{q}_j;\widehat{\mu}_i^t,\Sigma_i)}{\sum_{k=1}^{K}\mathcal{N}(\mathbf{q}_j;\widehat{\mu}_k^t,\Sigma_k)}. \tag{8}$$

Each of the soft-assignment-BoF of the sequence belongs to the unit simplex.

IV. Activity Representation and Recognition Using Simplex-HMM

Given an activity video, the proposed encoding represents the activity as a sequence of normalized BoF, $\mathcal{O} = \{O_1, \ldots, O_T\}$, each one belonging to the simplex $\Delta = \{\mathbf{v}_\lambda \in \mathbb{R}^K : v_{\lambda_i} \geq 0 : \sum_{k=1}^{K} v_{\lambda_k} = 1\}$. These observations are $\mathbb{R}^K$ vectors although the real dimensionality of the space is $(K-1)$. In Fig. 5(a), a simplex of 3-D is represented, and it can be observed that it is a triangle in a plane, so in reality it has only 2-D. The sequence of normalized BoF can be used for training a classifier based on HMM, suitable for modeling time sequences. The activity representation and recognition step shown in Fig. 1 depicts the flow chart of a classifier based on a modified HMM, which is explained later in this section.

Formally, the parameters of the HMM are $\theta = \{N, A, B, \pi\}$. N is the number of states, i.e., $S = \{S_1, \ldots, S_N\}$. Each observation, O_t is the emission produced by the hidden state z_t. The set of hidden states forms a sequence, $Z = \{z_1, \ldots, z_T\}$ where $z_t \in S$. $A = \{a_{ij}\}$ is the state transition matrix where a_{ij} represents the transition probability from state i to state j, $a_{ij} = p(z_{t+1} = S_j | z_t = S_i)$. $\pi = \{\pi_i\}$ is the initial state probability distribution where $\pi_i = p(z_1 = S_i)$, $1 \leq i \leq N$ being S_i the state at the beginning of the time series. Finally, B represents the observation probability distribution in every state where $b_j(O_t) = p(O_t \mid z_t = S_j)$. There are two main types of HMM based on the way the parameters in B are modeled: 1) the discrete HMM for categorical observations and 2) the continuous HMM, where a probability density function (PDF) is defined per state traditionally using a GMM. As previously mentioned, the observation space is the simplex Δ, which is a

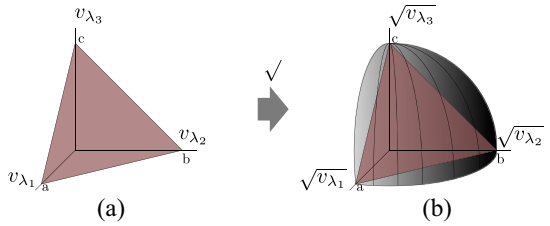

Fig. 5. (a) 3-D simplex representation and (b) unit sphere portion encompassing the square root transformation of the simplex.

continuous space. Therefore, the model should be a continuous HMM where the observations are vectors of real elements whose emission probability is traditionally approximated with a GMM per state.

In the simplex space, the emission probability can be modeled for instance with a Dirichlet distribution. However, the high dimensionality of the space causes numerical problems [45]. To exemplify these problems, we consider the simple case of a uniform distribution. In (9), we observe how a uniform distribution would require the PDF $f(\mathbf{x}) = (K-1)!, \mathbf{x} \in \Delta$, so that the integral in the simplex is 1. So, with a high K any PDF is numerically infeasible

$$\int_0^1 \int_0^{1-x_1} \cdots \int_0^{1-\sum_{i=1}^{K-2} x_i} (K-1)! d_{x_{K-1}} \ldots d_{x_2} d_{x_1} = 1. \quad (9)$$

The emission probability can be modeled in the $\mathbb{R}^K$ space, where there is no variance in the perpendicular dimension to the plane, or in a $\mathbb{R}^{K-1}$ space obtained for instance by performing the Aitchison's solution to the compositional data. However, both cases suffer for the same problem produced when samples have a high dimensionality and their number is limited for training. The lack of available data produces overfitting of the parameters, and the high dimensionality of the data intensifies the problem, so the training of any sort of parameter related to covariance is hopeless. We have corroborated this performance with some preliminary experiments with the continuous HMM and one Gaussian per state, obtaining numerical problems as the likelihood has always gone to $-\infty$.

In this paper, we propose to find a stable solution in spite of the high dimensionality. We simplify the observation model by defining the Euclidean distance between a mean vector and the observations, reducing the training parameters of the B function to only the means. Thus, we apply the observation model defined in

$$b_j(O_t) = e^{-\varphi \sqrt{\sum_{k=1}^{K} \left(v_{\lambda_k}^t - m_{jk}\right)^2}}. \quad (10)$$

Equation (10) shows φ and m_{jk} as free parameters but, as there are few samples in training and it is important to reduce as much as possible the parameters to learn, we experimentally fix the value of φ.

Although the function $b_j(O_t)$ is not a PDF it prevents the numerical problems while preserving the HMM properties thanks to the normalizations performed during the EM algorithm, as shown in (13) (see below). Moreover, the choice of the Euclidean distance in the exponential over a Gaussian comes from the experimental observation that a function highly peaked around data gives better results.

Considering that each $v_{\lambda_k}^t$ is an element in a histogram and represents the frequency of a specific feature model, it is possible to appreciate a drawback in the direct use of the Euclidean distance. Considering two normalized histograms of the same dimensionality, $A = \{a_i\}$ and $B = \{b_i\}$, $1 \leq i \leq N$, and $\sum_{i=1}^N a_i = \sum_{i=1}^N b_i = 1$, if $a_j = 1$, so $a_i = 0, \forall i \neq j$, and $b_j = 0$, then the dissimilarity between A and B should be maximum independent on the values of $b_i, \forall i \neq j$, and then the distance from A to B should remain constant for all values of $b_i, \forall i \neq j$. In Fig. 5(a), this distance would be represented by the distance from point a to any point in segment bc, which is not constant and the middle point of the segment is closer to a than the edges, being more significant with high dimensionality. To tackle this drawback, we propose to replace the Euclidean distance with the Hellinger distance, which is equivalent to transforming the points in the simplex to a portion of a hypersphere of unit radius by applying the square root of the vector element ($v_{\lambda_k}^t \rightarrow \sqrt{v_{\lambda_k}^t}$), as shown in Fig. 5(b). However, for the sake of simplicity we do not impose the condition that $\sum_{k=1}^K m_{jk} = 1$ in the optimization process. For the sake of clarity the transformed $\sqrt{v_{\lambda_k}}$ is not mentioned in the following equations because the formulation is equivalent to using v_{λ_k}, just changing one for the other and then the formulation is valid in both cases.

Given one, or several training observations, the HMM parameters can be estimated using the maximum likelihood through a Baum–Welch algorithm. This iterative estimation is obtained by maximizing the Baum's auxiliary function $Q(\hat{\theta}, \theta)$ [15], [46]

$$Q\left(\hat{\theta}, \theta\right) = \sum_Z p\left(Z|\mathcal{O}, \theta\right) \ln p\left(\mathcal{O}, Z|\hat{\theta}\right). \quad (11)$$

Defining $\gamma_t(i) = p(z_t = S_i|\mathcal{O}, \theta)$ and $\xi_t(i,j) = p(z_t = S_i, z_{t+1} = S_j|\mathcal{O}, \theta)$, the function Q can be expressed as

$$Q\left(\hat{\theta}, \theta\right) = \sum_{j=1}^N \gamma_1(j) \ln \pi_j + \sum_{t=1}^{T-1} \sum_{i=1}^N \sum_{j=1}^N \xi_t(i,j) \ln a_{ij} + \sum_{t=1}^T \sum_{j=1}^N \gamma_t(j) \ln\left(b_j(O_t)\right). \quad (12)$$

The EM algorithm followed requires a modification in the M step to optimize the function with respect to the proposed $b_j(O_t)$, which prevents from the problems arisen with scarce data. This special case is presented below.

A. E-Step

This step implies the calculation of functions $\xi_t(i,j)$ and $\gamma_t(i)$. They are calculated with the standard equations for a general observation model $b_j(O_t)$

$$\xi_t(i,j) = \frac{\alpha_t(i) a_{ij} b_j(O_{t+1}) \beta_{t+1}(j)}{\Sigma_{i=1}^N \Sigma_{j=1}^N \alpha_t(i) a_{ij} b_j(O_{t+1}) \beta_{t+1}(j)} \quad (13)$$

where $\alpha_t(i) = p(O, z_t = S_i|\theta)$ and $\beta_t(j) = p(O|\theta, z_t = S_j)$ are auxiliary probabilities calculated by the forward and backward algorithms [15]. Equation (13) is computed using the proposed $b_j(O_{t+1})$.

Finally, $\gamma_t(i)$ is obtained with

$$\gamma_t(i) = \sum_{j=1}^{N} \xi_t(i,j). \tag{14}$$

B. M-Step

This process calculates the $\hat{\pi}_i$, $\hat{a}_{ij}$, and $\hat{m}_{jk}$ that maximize $Q(\hat{\theta}, \theta)$. The optimizations of $\hat{\pi}_i$, $\hat{a}_{ij}$, and $\hat{m}_{jk}$ are obtained by maximizing (12). In our method the optimizations of $\hat{\pi}_i$ and $\hat{a}_{ij}$ are the same as in the traditional method but $\hat{m}_{jk}$ should be computed differently as its term changes in the mentioned equation. Therefore, (15) has to be maximized with respect to m_{jk}

$$\sum_t \sum_j \gamma_t(j) \ln\left(b_j(O_t)\right) = \sum_t \sum_j \gamma_t(j) \left(-\varphi \sqrt{\sum_{k=1}^{K} \left(v_{\lambda_k}^t - m_{jk} \right)^2} \right). \tag{15}$$

By setting $(\partial / \partial m_{jk}) = 0$, the following equation is obtained:

$$\varphi \sum_{t=1}^{T} \gamma_t(j) \frac{\left(v_{\lambda_k}^t - m_{jk} \right)}{\sqrt{\sum_{k'=1}^{K} \left(v_{\lambda_{k'}}^t - m_{jk'} \right)^2}} = 0. \tag{16}$$

Since m_{jk} does not depend on t and $\gamma_t(j)$ are treated as constants in the M-step once computed in the E-step, (17) can be easily derived

$$m_{jk} = \frac{\sum_{t=1}^{T} \gamma_t(j) \dfrac{v_{\lambda_k}^t}{\sqrt{\sum_{k'=1}^{K} \left(v_{\lambda_{k'}}^t - m_{jk'} \right)^2}}}{\sum_{t=1}^{T} \gamma_t(j) \dfrac{1}{\sqrt{\sum_{k'=1}^{K} \left(v_{\lambda_{k'}}^t - m_{jk'} \right)^2}}}. \tag{17}$$

Then, since m_{jk} is on the left and on the right side, the equation is solved by a fixed point iteration, obtaining $\hat{m}_{jk}$ when convergence is achieved.

Each SHMM trained with a single video has a specific GMM computed with the MAP adaptation, so the SHMM model is defined by $\Gamma(A, B, \pi, \widehat{\mu}_i, \Sigma_i)$. As each training sequence is modeled with an SHMM the inclusion of new training sequences implies a linear increment on the storage space and the required computational power for testing.

V. Experiments and Results

A. Datasets

This paper focuses on human activity recognition applied on constrained scenarios, where videos are obtained by fixed viewpoint cameras. The proposed algorithm is trained using human motion information from external video sources using MAP adaptation, as described in Section III-B. Our method is evaluated using several datasets that accomplish the source and target domain constraints. We have selected three source domain datasets that include a high variability in unconstrained video clips that simulate the easily obtainable ones from the Internet. On the other hand, we have selected three popular datasets in the human activity recognition field as target domain where the videos are recoded from fixed cameras. Additionally, a dataset with unconstrained video recording has been selected as target dataset in order to evaluate the performance of the algorithm in general purpose applications.

Fig. 6. Target domain datasets: Weizmann (1st row), KTH (2nd row), and IXMAS (3rd row).

1) Source Domain Datasets: Three public and extensive datasets, HMDB51 [1], OlympicSprots [2], and Virat Release 2.0 [47], are used as source domain. They include a high variability of movements in several locations. The three datasets combined have 79 different activity classes extracted from YouTube, movies or surveillance cameras in 7878 video clips.

2) Target Domain Datasets: The Weizmann dataset [3] is composed by 93 low-resolution (180×144, 50 frames/s) video sequences showing nine different people, each performing ten natural activities: 1) *Bend*; 2) *Jumping-Jack*; 3) *Jump-Forward-on-Two-Legs*; 4) *Jump-in-Place-on-Two-Legs*; 5) *Run*; 6) *Gallop-Side-Ways*; 7) *Skip*; 8) *Walk*; 9) *Wave-One-Hand*; and 10) *Wave-Two-Hands*. The IXMAS dataset [5] is composed by five camera viewpoints (390×291, 23 frames/s) of 11 actors performing three times each of the 13 activities included: 1) *Check-Watch*; 2) *Cross-Arms*; 3) *Scratch-Head*; 4) *Sit-Down*; 5) *Get-Up*; 6) *Turn-Around*; 7) *Walk*; 8) *Wave*; 9) *Punch*; 10) *Kick*; 11) *Point*; 12) *Pick-Up*; and 13) *Throw*. The KTH dataset [4] has been captured in four different scenarios where static cameras have recorded, at low-resolution (160 × 120, 25 frames/s), 25 subjects performing several times six types of activities: 1) *Walking*; 2) *Jogging*; 3) *Running*; 4) *Boxing*; 5) *Hand-Waving*; and 6) *Hand-Clapping*. Frame examples of these datasets are shown in Fig. 6. Finally, we have selected the UCF11 dataset [48] composed by unconstrained video clips of 11 categories obtained from YouTube.

All videos are processed by means of the state-of-the-art IDT[1] extractor. From the IDTs extracted from the source domain datasets, 100 000 are randomly selected and used for the GMM training, obtaining 5000 Gaussians, which represent

[1]IDT descriptor code can be downloaded in http://lear.inrialpes.fr/people/wang/download/improved_trajectory_release.tar.gz.

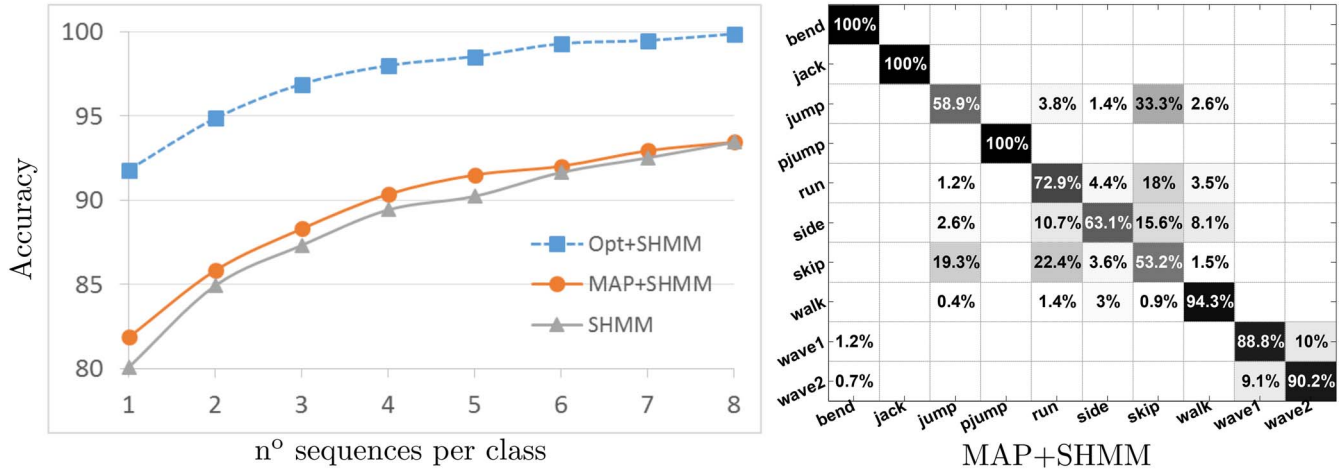

Fig. 7. Strict one-shot learning results in Weizmann dataset. Left: accuracy obtained with different number of training examples per class. Right: confusion matrix of the MAP+SHMM method using only one example per class in training.

the UBM vocabulary. Below we detail the performed experiments using two approaches: 1) strict one-shot learning and 2) relaxed one-shot learning.

B. Strict One-Shot Learning

Considering the proposed activity representation, there are two possible ways of modeling an activity. First, the simplest and fastest method uses the original UBM trained with the source datasets, which is represented by a GMM $\lambda = \{\mu_i, \Sigma_i\}$. An SHMM is then trained per example obtaining the model $\Gamma(A, B, \pi, \mu_i, \Sigma_i)$ where μ_i and Σ_i is shared in all models. We define the SHMM as an ergodic two-state model and set $\varphi = 1.5$, as experiments shown that the performance is rather insensitive when φ is in the range $(1, 2)$. The second approach, on the other hand, adapts the UBM vocabulary to an improved GMM per example using the explained MAP adaptation. Reynolds *et al.* [10] suggested the insensitivity of the method to the parameter r that we experimentally corroborate, selecting finally $r = 0.014$, where only the mean is modified. Again, an SHMM is trained per activity example, but each activity model is represented in the adapted UBM vocabulary, which implies different GMM means per example as specific information and only Σ_i is shared among models, $\widehat{\Gamma}(A, B, \pi, \widehat{\mu}_i, \Sigma_i)$. This second approach is called MAP+SHMM in the experiments.

In addition to the previous representations, a special instance of the SHMM approach is performed in Weizmann dataset in order to validate the proposed algorithms. If the source dataset used to train the UBM is the whole target domain, including both, train and test examples, then the obtained UBM is the optimal that can be reached with the method configuration, so this special case is considered the UBM ground truth and is labeled with the name Opt+SHMM in the experiments. It is worth noting that in a real world application this is infeasible and the Opt+SHMM configuration is only used to represent the experimental ceiling of our methodology.

We perform the following initialization for the EM algorithm used in the SHMM with two states: 1) $\pi_1 = 1$ and 2) $\pi_2 = 0$, the transition matrix is randomly initialized, and finally the initial mean vectors, $\mathbf{m}_1$ and $\mathbf{m}_2$, are the observations closest to times $((T-1)/4)+1$ and $((3(T-1))/4)+1$ of the training sequence.

The experiments in this section are conducted as follows. Using one-subject-out model, num training sequences per class are randomly selected from the remaining subjects. The value of num goes from 1 to the maximum available sequences. The result per subject are the average of 100 runs, and the final result is the average of all subjects.

Fig. 7 shows on the left a graph with the performance of the method proposed in this paper using the three activity representations described previously. It is worth noting the Opt+SHMM results because they justify the suitability of the selected activity representation, i.e., the IDT features encoded in a sequence of BoFs which trains an SHMM. The results are impressive with only one sequence of each class, as it reaches a 91.8%, and when using the eight sequences available it almost reaches the 100%, which is comparable to the state-of-the-art results. However, as explained before, this is only possible if the feature space is properly modeled with a GMM, and in this case we have used information from the whole dataset. We can conclude from this result that a proper feature space representation becomes an important objective to be achieved. Thus, we have trained a UBM vocabulary, represented with a GMM of IDTs, obtained from a set of videos as diverse as possible (using the three source domain datasets). Applying the SHMM configuration with the GMM trained with three source datasets, the method performance falls significantly against the Opt+SHMM configuration, although it still obtains a satisfactory 80.11% using only one sequence per class. Finally,the results are improved by adapting the GMM to the scenario, but as each model uses a single example available, the MAP adaptation has to be performed to this limited available data using the MAP+SHMM configuration. Fig. 7 demonstrates how this adaptation improves the results during all the series, which implies that the adaptation to the target scenario improves the features representation. On the right of Fig. 7, the confusion matrix of the MAP+SHMM method using only one sequence for training is depicted. From all the classes the greatest confusion is produced among activities that

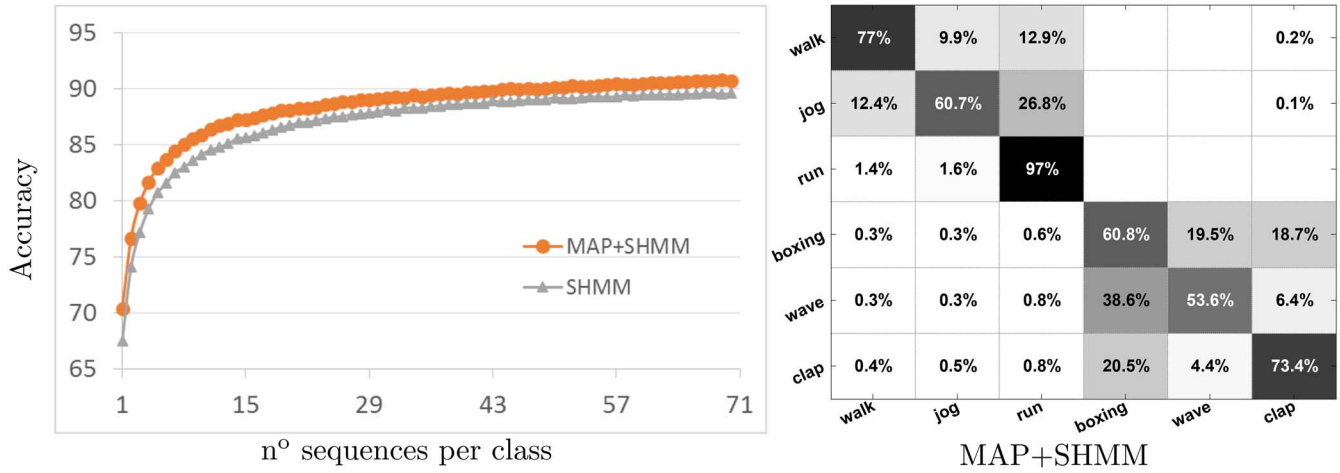

Fig. 8. Strict one-shot learning results in KTH dataset. Left: accuracy obtained with different number of training examples per class. Right: confusion matrix of the MAP+SHMM method using only one example per class in training.

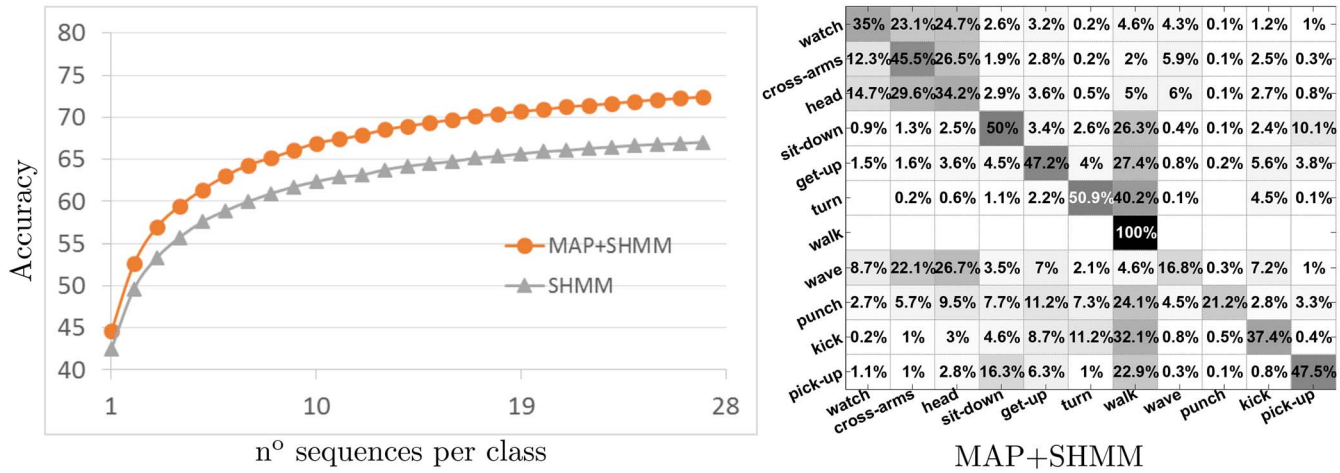

Fig. 9. Strict one-shot learning results in IXMAS dataset. Left: accuracy obtained with different number of training examples per class. Right: confusion matrix of the MAP+SHMM method using only one example per class in training.

involve subject displacement (*Jump, Run, Side, Skip*), caused by the model giving more importance to the displacement information than the limbs movements. Some works as the one in [3] incorporates a preprocessing that compensates the displacement, but because of the use of background subtraction and its complications in some scenarios we have opted to Avoid it.

Fig. 8 shows the performance of our proposed method on KTH dataset, only including results for SHMM and MAP+SHMM representations. In this case there are up to 70 examples for training, and as the graph shows there is a constant gap between SHMM and MAP+SHMM almost independent on the training examples, which clearly demonstrates the improvement obtained using the proposed adaptation to the scenario. Attending to the confusion matrix we can observe the same phenomenon produced in Weizmann dataset, the classes with displacement (*Walk, Jog, Run*) are mainly confused among them. Additionally, we observe in this dataset how the "static" classes (*Boxing, Wave, Clap*) are confused as well among them. Unlike Weizmann, the static activities in KTH are all described by the movement of the subject arms, which results to the difficulty to distinguish them.

Finally, we repeat the experiments using the IXMAS dataset but avoiding the point and throw activities as suggested in [5] and Fig. 9 shows these results. It is worth noting that IXMAS dataset is recorded simultaneously with five fixed cameras each one with different viewpoint. We conduct the experiment separately per camera and the shown results is the average of these experiments. Due to the free subject position in the scenario some activities, like *Check-Watch, Cross-Arms* but also others, are occluded by the subject body in some cameras generating a worse performance in comparison to the other datasets. However, we ratify the suitability of the MAP adaptation in the graph. The confusion matrix highlights two phenomena. First, the *Walk* activity is always right but several other activities are confused with it, which indicates a bias in that model that could be compensated but potential solution is beyond the scope of this paper. Second, there are four activities (*Check-Watch, Cross-Arms, Scratch-Head*, and *Wave*) that are mainly confused among them. The lower amount of movement in these activities contributes to a higher dependence in the camera viewpoint and therefore their confusion.

As the experiments in IXMAS have been performed per camera we can evaluate them separately. The results of each

TABLE I
ACCURACY USING STRICT ONE-SHOT LEARNING IN EACH OF THE IXMAS CAMERAS USING 1 AND 27 EXAMPLES FOR TRAINING

	camera1		camera2		camera3		camera4		camera5	
	1	27	1	27	1	27	1	27	1	27
SHMM	45.7	73.6	44.5	71.5	43.1	69.7	48.5	69.7	30.6	50.6
MAP+SHMM	48.3	78.5	45.8	76.1	44.7	71.5	50	74.8	34	61.2

TABLE II
STRICT ONE-SHOT LEARNING WITH ONE EXAMPLE PER CLASS

	Weizmann	KTH	IXMAS
FDHMM [36]	68.17%	67.16%	25.36%
MAP+FDHMM [36]	69.61%	67.6%	33.7%
SHMM	80.11%	67.53%	42.47%
MAP+SHMM	**81.88%**	**70.39%**	**44.58%**
Seo and Milanfar [6]	75%	65%	-
Rodriguez et al. [9]	-	-	35%*

*Not directly comparable as they use only one camera and 5 initial sequences, which is less restrictive.
(-) Lack of results in the referenced papers.

TABLE III
STRICT ONE-SHOT LEARNING FOR UCF11 DATASET. RESULTS FOR OUR APPROACH COMPARED WITH [7]

	1	10	20	30	40	50
SHMM	30.7%	59.2%	69%	75%	79.2%	82%
Yang et al. [7]	19.3%	31.3%	39.2%	46.3%	50%	51%

TABLE IV
RELAXED ONE-SHOT LEARNING WITH ONE EXAMPLE PER CLASS. RESULTS OF OUR APPROACH AND TWO STATE-OF-THE-ART METHODS

	Weizmann	KTH	IXMAS
SHMM	84.18%	76.65%	52.84%
MAP+SHMM	**87.12%**	**80.21%**	**56.43%**
Yang et al. [7]	80%	-	-
Orrite et al. [8]	81.1%	-	-

(-) Lack of results in the referenced papers.

camera accuracy is shown in Table I using only one example per training class or using the maximum of 27. In addition to the MAP+SHMM improvement, we can highlight that this improvement is more significant in camera 5, which is a zenith camera. The viewpoint of this camera is rarely used and then the movements are worse represented in the UBM. Thus, the MAP adaptation produces a greater impact.

We have found only one paper covering the strict one-shot learning paradigm [6], although indirectly. They propose a sequence representation based on their defined local space-time descriptors. Afterwards, computing a distance among sequences they select the class of the closest one, being a strict one-shot learning as the representation do not need information of other sequences. The experimental results are presented by two graphs, one for Weizmann and other for KTH, that show the performance obtained using only one sequence per class in the training. In Table II, we compare our results with this paper, extracting their results approximately from the graphs, showing clearly how our approach improves the previous results significantly in the two comparable datasets. In IXMAS, we compare with [9], where silhouettes ware used as descriptors. In that work, only camera1 was used, starting with five sequences and not only one, although they studied the performance including new classes, which approximates the method to strict one-shot learning. The proposed method clearly overcame their results using the five cameras (camera5 gives the worst results), and learning from the first sequence. Moreover, in Section II, we have mentioned FDHMM [36] which is able to train a stable HMM from a single sequence of vectors in a unit simplex, as our proposal does. However, the histogram distribution is not considered and therefore it fails in the experiments as shown in Table II where we conduct the FDHMM experiments with and without the MAP adaptation.

After proving the suitability of the method for constrained scenarios, we evaluate the strict one-shot learning in the unconstrained dataset UCF11. We randomly chose 1, 10, 20, 30, 40, and 50 video-clips of each class for training and we test the rest. The average of 50 runs is the result shown in Table III. This experiment is comparable to the results found in [7]. Initially, when choosing one sequence for training, we compare SHMM with MAP–SHMM, obtaining similar results (30.67% and 30.83%, respectively). As sequences belong to unconstrained scenarios the UBM adaptation does not improve the accuracy and we discard it. On the other hand, we verify how our approach has a good performance compared with [7].

C. Relaxed One-Shot Learning

As the literature is scarce in one-shot learning methods for human activity recognition, we add a new experiment using the relaxed one-shot learning methodology. In this experiment, we select the video examples of one subject, and from them only one example per class. These examples are used for training one SHMM per class, and all the other subjects are used in testing. The relaxed one-shot learning allows us to apply the MAP adaptation to the features extracted from all the training examples, which implies a better adaptation in comparison to the previous experiments. Moreover, the GMM is now shared among the SHMMs as in the SHMM method. However, this process has some constraints in comparison to the strict methodology as a sequence per class is necessary from the beginning, which initially can be expensive to obtain, and implies a less flexible addition of new examples and classes.

Table IV shows the results in relaxed one-shot learning using our method in comparison with some results found in the literature. In [7], spatio-temporal subactions based on optical flow are defined and modeled from all the sequences available for training. In [8], the descriptors are MHIs [19] based on silhouettes computed in a fixed temporal window. MHIs from all the sequences in training are used to model the feature space.

TABLE V
ACCURACY OF THE PROPOSED METHOD WITH SEVERAL TRAINING EXAMPLES, IN COMPARISON WITH STATE-OF-THE-ART RESULTS

	Weizmann	KTH	IXMAS
OneOut+SHMM	98.9%	94.2%	82.5%
Liu et al. [49]	100%	94.8%	95.5%

Both methods are outperformed, demonstrating the suitability of the proposed method. Again, it is shown the improvement achieved by the use of the MAP adaptation to the scenario. The improvement of these results compared to the strict methodology happens not only because of the adaptation, as the SHMM method does not benefit from it, but also because every SHMM uses the same actor, and therefore the difference is not on the actor features but only on the activity.

In Figs. 7–9, we have shown the evolution of the method performance while increasing the number of labeled examples. However, when many training sequences are available the MAP adaptation to each sequence is not optimal as there is enough information for training a specific GMM. Therefore, using a leave-one-person-out cross validation methodology we have carried out a new experiment. Obtaining a GMM per person with the examples of the remaining subjects, making unnecessary any adaptation, we have trained an SHMM per example, keeping unchanged the rest of the system. We call this new experiment OneOut-SHMM. As shown in Table V, our method achieves almost state-of-the-art results in Weizmann and KTH, being the gap of Weizmann caused by only one sequence misclassified. However, in IXMAS we obtain worse results, probably partially caused by a naive fusion of cameras, we have selected the class of the HMM producing the highest likelihood among all cameras. These results show how the method, although performing reasonably well with several training data, it is not the best suited for this task.

VI. CONCLUSION

The human activity representation proposed in this paper has been proved suitable in activity recognition in fixed-background constrained scenarios with very few available training examples. The introduced SHMM facilitates the modeling of an activity using limited amount of data, as few as one example per class, thanks to the reduction of parameters to train, exploiting the proposed simplex constraints of the samples. In the Weizmann experiments, we have seen how these representation obtains great results if the feature space is properly modeled with a GMM.

In order to obtain the best representation of the feature space using a GMM, but taking into account the limited data available in the target scenario, we propose an adaptation of a UBM trained in source datasets. We have proved how an adaptation of the UBM to the target domain information modeled only with one example in the target scenario improves the results obtained using directly the original UBM. The results obtained in the Transfer Learning stage demonstrate the value of the proposed method adopted, but also that there is still scope of improvement in future work.

It is worth noting that the proposed algorithm assumes a limited number of available labeled sequences from the target dataset. However, the more labeled sequences, the more storage space and computational power is required for inferring sequences. Therefore, in cases where more data is available, other existing algorithms may be more practical and effective as shown in the experiments.

Also, it is worth noting the shortage of relevant work in the literature existing in one-shot learning for human activities. Especially in the strict one-shot learning paradigm very little work has been done, and our point of view is that it is the most appropriate in many real life applications, thanks to its flexibility including new examples and classes. Although the human activity recognition community is tending to focus in large unconstrained datasets, more research in this field can accelerate the installation of recognition systems in new scenarios.

REFERENCES

[1] H. Kuehne, H. Jhuang, E. Garrote, T. Poggio, and T. Serre, "HMDB: A large video database for human motion recognition," in *Proc. IEEE Int. Conf. Comput. Vis. (ICCV)*, Barcelona, Spain, 2011, pp. 2556–2563.

[2] J. C. Niebles, C.-W. Chen, and L. Fei-Fei, "Modeling temporal structure of decomposable motion segments for activity classification," in *Proc. Eur. Conf. Comput. Vis. (ECCV)*, Heraklion, Greece, 2010, pp. 392–405.

[3] L. Gorelick, M. Blank, E. Shechtman, M. Irani, and R. Basri, "Actions as space-time shapes," *IEEE Trans. Pattern Anal. Mach. Intell.*, vol. 29, no. 12, pp. 2247–2253, Dec. 2007.

[4] C. Schuldt, I. Laptev, and B. Caputo, "Recognizing human actions: A local SVM approach," in *Proc. 17th Int. Conf. Pattern Recognit. (ICPR)*, Cambridge, U.K., 2004, pp. 32–36. [Online]. Available: http://www.nada.kth.se/cvap/actions/

[5] D. Weinland, R. Ronfard, and E. Boyer, "Free viewpoint action recognition using motion history volumes," *Comput. Vis. Image Understand.*, vol. 104, nos. 2–3, pp. 249–257, 2006. [Online]. Available: http://4drepository.inrialpes.fr/public/viewgroup/6

[6] H. J. Seo and P. Milanfar, "Action recognition from one example," *IEEE Trans. Pattern Anal. Mach. Intell.*, vol. 33, no. 5, pp. 867–882, May 2011. [Online]. Available: http://doi.ieeecomputersociety.org/10.1109/TPAMI.2010.156

[7] Y. Yang, I. Saleemi, and M. Shah, "Discovering motion primitives for unsupervised grouping and one-shot learning of human actions, gestures, and expressions," *IEEE Trans. Pattern Anal. Mach. Intell.*, vol. 35, no. 7, pp. 1635–1648, Jul. 2013.

[8] C. Orrite, M. Rodríguez, and M. Montañés, "One-sequence learning of human actions," in *Human Behavior Understanding*, vol. 7065, A. A. Salah and B. Lepri, Eds. Heidelberg, Germany: Springer, 2011, pp. 40–51.

[9] M. Rodríguez, C. Medrano, E. Herrero, and C. Orrite, "Transfer learning of human poses for action recognition," in *Human Behavior Understanding*. Cham, Switzerland: Springer, 2013, pp. 89–101.

[10] D. A. Reynolds, T. F. Quatieri, and R. B. Dunn, "Speaker verification using adapted Gaussian mixture models," *Digit. Signal Process.*, vol. 10, nos. 1–3, pp. 19–41, 2000.

[11] H. Wang and C. Schmid, "Action recognition with improved trajectories," in *Proc. IEEE Int. Conf. Comput. Vis. (ICCV)*, Sydney, NSW, Australia, 2013, pp. 3551–3558.

[12] I. Laptev, M. Marszalek, C. Schmid, and B. Rozenfeld, "Learning realistic human actions from movies," in *Proc. IEEE Conf. Comput. Vis. Pattern Recognit. (CVPR)*, Anchorage, AK, USA, Jun. 2008, pp. 1–8.

[13] N. Dalal, B. Triggs, and C. Schmid, "Human detection using oriented histograms of flow and appearance," in *Proc. Eur. Conf. Comput. Vis. (ECCV)*, Graz, Austria, 2006, pp. 428–441.

[14] T. Shinozaki and M. Ostendorf, "Cross-validation and aggregated EM training for robust parameter estimation," *Comput. Speech Lang.*, vol. 22, no. 2, pp. 185–195, 2008.

[15] L. R. Rabiner, "A tutorial on hidden Markov models and selected applications in speech recognition," *Proc. IEEE*, vol. 77, no. 2, pp. 257–286, Feb. 1989.

[16] P. Turaga, R. Chellappa, V. S. Subrahmanian, and O. Udrea, "Machine recognition of human activities: A survey," *IEEE Trans. Circuits Syst. Video Technol.*, vol. 18, no. 11, pp. 1473–1488, Nov. 2008.

[17] R. Poppe, "A survey on vision-based human action recognition," *Image Vis. Comput.*, vol. 28, no. 6, pp. 976–990, Jun. 2010.
[18] D. Weinland, R. Ronfard, and E. Boyer, "A survey of vision-based methods for action representation, segmentation and recognition," *Comput. Vis. Image Understand.*, vol. 115, no. 2, pp. 224–241, Feb. 2011.
[19] A. Bobick and J. Davis, "Real-time recognition of activity using temporal templates," in *Proc. 3rd IEEE Workshop Appl. Comput. Vis. (WACV)*, Sarasota, FL, USA, Dec. 1996, pp. 39–42.
[20] A. F. Bobick and J. W. Davis, "The recognition of human movement using temporal templates," *IEEE Trans. Pattern Anal. Mach. Intell.*, vol. 23, no. 3, pp. 257–267, Mar. 2001.
[21] A. Yilmaz and M. Shah, "Actions sketch: A novel action representation," in *Proc. IEEE Conf. Comput. Vis. Pattern Recognit. (CVPR)*, vol. 1. San Diego, CA, USA, Jun. 2005, pp. 984–989.
[22] D. G. Lowe, "Distinctive image features from scale-invariant keypoints," *Int. J. Comput. Vis.*, vol. 60, no. 2, pp. 91–110, Nov. 2004.
[23] I. Laptev, "On space-time interest points," *Int. J. Comput. Vis.*, vol. 64, nos. 2–3, pp. 107–123, Sep. 2005.
[24] P. Dollar, V. Rabaud, G. Cottrell, and S. Belongie, "Behavior recognition via sparse spatio-temporal features," in *Proc. 14th Int. Conf. Comput. Commun. Netw. (ICCCN)*, San Diego, CA, USA, 2005, pp. 65–72.
[25] O. Kliper-Gross, Y. Gurovich, T. Hassner, and L. Wolf, "Motion interchange patterns for action recognition in unconstrained videos," in *Proc. Eur. Conf. Comput. Vis. (ECCV)*, Florence, Italy, 2012, pp. 256–269.
[26] D. Oneata, J. Verbeek, and C. Schmid, "Action and event recognition with Fisher vectors on a compact feature set," in *Proc. IEEE Int. Conf. Comput. Vis. (ICCV)*, Sydney, NSW, Australia, 2013, pp. 1817–1824.
[27] H. Wang, A. Kläser, C. Schmid, and C.-L. Liu, "Dense trajectories and motion boundary descriptors for action recognition," *Int. J. Comput. Vis.*, vol. 103, no. 1, pp. 60–79, 2013.
[28] D. Batra, T. Chen, and R. Sukthankar, "Space-time shapelets for action recognition," in *Proc. IEEE Workshop Motion Video Comput. (WMVC)*, Jan. 2008, pp. 1–6.
[29] A. Veeraraghavan, A. K. Roy-Chowdhury, and R. Chellappa, "Matching shape sequences in video with applications in human movement analysis," *IEEE Trans. Pattern Anal. Mach. Intell.*, vol. 27, no. 12, pp. 1896–1909, Dec. 2005.
[30] B. Yao and S.-C. Zhu, "Learning deformable action templates from cluttered videos," in *Proc. IEEE Int. Conf. Comput. Vis. (ICCV)*, Kyoto, Japan, 2009, pp. 1507–1514.
[31] C. Sminchisescu, A. Kanaujia, and D. Metaxas, "Conditional models for contextual human motion recognition," *Comput. Vis. Image Understand.*, vol. 104, nos. 2–3, pp. 210–220, Nov./Dec. 2006.
[32] J. D. Lafferty, A. McCallum, and F. C. N. Pereira, "Conditional random fields: Probabilistic models for segmenting and labeling sequence data," in *Proc. 8th Int. Conf. Mach. Learn.*, Williamstown, MA, USA, 2001, pp. 282–289.
[33] A. Quattoni, S. Wang, L.-P. Morency, M. Collins, and T. Darrell, "Hidden conditional random fields," *IEEE Trans. Pattern Anal. Mach. Intell.*, vol. 29, no. 10, pp. 1848–1852, Oct. 2007.
[34] X. Feng and P. Perona, "Human action recognition by sequence of movelet codewords," in *Proc. 1st Int. Symp. 3D Data Process. Vis. Transm.*, Padua, Italy, 2002, pp. 717–721.
[35] W.-L. Lu and J. J. Little, "Simultaneous tracking and action recognition using the PCA-HOG descriptor," in *Proc. 3rd Can. Conf. Comput. Robot Vis.*, Jun. 2006, p. 6.
[36] H. Uğuz, A. Öztürk, R. Saraçoğlu, and A. Arslan, "A biomedical system based on fuzzy discrete hidden Markov model for the diagnosis of the brain diseases," *Expert Syst. Appl.*, vol. 35, no. 3, pp. 1104–1114, Oct. 2008.
[37] S. J. Pan and Q. Yang, "A survey on transfer learning," *IEEE Trans. Knowl. Data Eng.*, vol. 22, no. 10, pp. 1345–1359, Oct. 2010.
[38] D. Cook, K. D. Feuz, and N. C. Krishnan, "Transfer learning for activity recognition: A survey," *Knowl. Inf. Syst.*, vol. 36, no. 3, pp. 537–556, 2013.
[39] J. Liu, M. Shah, B. Kuipers, and S. Savarese, "Cross-view action recognition via view knowledge transfer," in *Proc. IEEE Conf. Comput. Vis. Pattern Recognit. (CVPR)*, Providence, RI, USA, 2011, pp. 3209–3216.
[40] W. Bian, D. Tao, and Y. Rui, "Cross-domain human action recognition," *IEEE Trans. Syst., Man, Cybern. B, Cybern.*, vol. 42, no. 2, pp. 298–307, Apr. 2012.
[41] Y. Zhu, X. Zhao, Y. Fu, and Y. Liu, "Sparse coding on local spatial-temporal volumes for human action recognition," in *Proc. Asian Conf. Comput. Vis. (ACCV)*, Queenstown, New Zealand, 2010, pp. 660–671.
[42] D. H. Hu, V. W. Zheng, and Q. Yang, "Cross-domain activity recognition via transfer learning," *Pervasive Mobile Comput.*, vol. 7, no. 3, pp. 344–358, Jun. 2011.
[43] L. Fei-Fei, R. Fergus, and P. Perona, "One-shot learning of object categories," *IEEE Trans. Pattern Anal. Mach. Intell.*, vol. 28, no. 4, pp. 594–611, Apr. 2006.
[44] L. Cao, Z. Liu, and T. S. Huang, "Cross-dataset action detection," in *Proc. IEEE Conf. Comput. Vis. Pattern Recognit. (CVPR)*, San Francisco, CA, USA, 2010, pp. 1998–2005.
[45] T. P. Minka, "Estimating a Dirichlet distribution," Mach. Intell. Perception Group, Microsoft Res., Cambridge, U.K., Tech. Rep., 2009. [Online]. Available: http://research.microsoft.com/en-us/um/people/minka/papers/dirichlet/minka-dirichlet.pdf
[46] C. M. Bishop, *Pattern Recognition and Machine Learning* (Information Science and Statistics). New York, NY, USA: Springer, 2006. [Online]. Available: http://www.springer.com/us/book/9780387310732
[47] S. Oh *et al.*, "A large-scale benchmark dataset for event recognition in surveillance video," in *Proc. IEEE Conf. Comput. Vis. Pattern Recognit. (CVPR)*, Providence, RI, USA, 2011, pp. 3153–3160.
[48] J. Liu, J. Luo, and M. Shah, "Recognizing realistic actions from videos 'in the wild,"' in *Proc. IEEE Conf. Comput. Vis. Image Understand. (CVPR)*, Miami, FL, USA, 2009, pp. 1996–2003.
[49] L. Liu, L. Shao, X. Zhen, and X. Li, "Learning discriminative key poses for action recognition," *IEEE Trans. Cybern.*, vol. 43, no. 6, pp. 1860–1870, Dec. 2013.

Mario Rodriguez received the M.Eng. degrees in telecommunications engineering and biomedical engineering from the University of Zaragoza, Zaragoza, Spain, in 2007 and 2009, respectively, where he is currently pursuing the Ph.D. degree.

He belongs to the Computer Vision Laboratory Group, Aragon Institute for Engineering Research, University of Zaragoza. His current research interests include computer vision, machine learning and pattern recognition, especially focused in human activity understanding.

Carlos Orrite (M'06) received the M.Eng. degree in industrial engineering, the M.Sc. degree in biomedical engineering (specializing in medical instrumentation), and the Ph.D. degree in computer vision from the University of Zaragoza, Zaragoza, Spain, in 1989, 1994, and 1997, respectively.

He is currently an Associate Professor with the Department of Electronics and Communications Engineering, University of Zaragoza, where he also carries out his research activities with the Aragon Institute of Engineering Research as an Associate Director. His current research interests include computer vision and machine learning.

Carlos Medrano (SM'11) received the Ph.D. degree in physics jointly from the University of Zaragoza, Zaragoza, Spain, and Joseph Fourier University, Grenoble, France, in 1997.

He has been with the Department of Electronic and Communications Engineering, University of Zaragoza, since 1998, where he is a Tenured Faculty Member. He has a broad research career including topics such as magnetism, data acquisition and control systems, and computer vision. He has authored over 25 papers in peer-reviewed journals and many conference contributions. His current research interests include pattern recognition, with applications to action recognition from videos and to the discovery of patterns in data recorded with wearable sensors, specially for health applications.

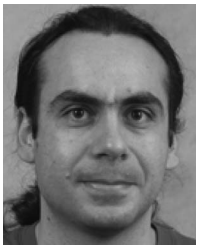

Dimitrios Makris (M'03) received the Diploma degree in electrical and computer engineering from the Aristotle University of Thessaloniki, Thessaloniki, Greece, in 1999, and the Ph.D. degree in computer vision from City University, London, U.K., in 2004.

He is currently an Associate Professor with the School of Computer Science and Mathematics, Kingston University, London. His current research interests include image processing, computer vision and machine learning, and particularly motion analysis.

Dr. Makris is currently the Vice Chair of the IET Vision and Imaging Network and a member of the British Machine Vision Association.